

# The Electrochromic Properties of an Alternative Copolymer Containing benzo[1,2-b:4,5-b']dithiophene as the Electron Donor and Benzoselenadiazole as the Electron Acceptor Units

Shuang Chen<sup>1,2</sup>, Qi Ji<sup>3</sup>, Lingqian Kong<sup>4</sup>, Xiuping Ju<sup>4</sup>, Jinsheng Zhao<sup>2\*</sup>

<sup>1</sup>Department of Chemical Engineering, China University of Petroleum (East China), QingDao, 266580, P. R. China

<sup>2</sup> Shandong Key Laboratory of Chemical Energy-storage and Novel Cell Technology, Liaocheng University, 252059, Liaocheng, P. R. China

<sup>3</sup>College of Chemistry and Environmental Science, Hebei University, Baoding, 071002, P. R. China

<sup>4</sup>Dongchang colledge, Liaocheng University, 252059, Liaocheng, P. R. China

\*E-mail: [j.s.zhao@163.com](mailto:j.s.zhao@163.com)

Received: 9 February 2017 / Accepted: 28 February 2017 / Published: 12 March 2017

One novel electrochromic copolymer, poly(benzo[1,2-b:4,5-b']dithiophene-benzoselenadiazole) (PBDTBS) was synthesized successfully by chemical polymerization. Afterwards, some characterizations were carried out, including electrochemistry, spectroelectrochemistry, density functional theory(DFT) calculation, kinetics and thermal gravimetric analysis. When the copolymer is oxidized, it changes from greyish-green to darkgrey. The band gap of the copolymer calculated according to the onset wavelength of the optical absorption band is 1.55 eV. The optical contrast of the copolymer are 14.0 % at 450 nm, 9.0 % at 670 nm and 30.7 % at 1560 nm. The coloration efficiency are  $60.61\text{cm}^2\cdot\text{C}^{-1}$  at 450 nm,  $84.60\text{ cm}^2\cdot\text{C}^{-1}$  at 670 nm and  $135.84\text{cm}^2\cdot\text{C}^{-1}$  at 1560 nm. The decomposition temperature is 344 °C. It can be a candidate for the electrochromic application.

**Keywords:** conducting polymers, donor-acceptor type, benzo[1,2-b:4,5-b']dithiophene, benzoselenadiazole.

## 1. INTRODUCTION

In the past few years, conducting copolymers have developed quickly due to their wide application in organic light-emitting diodes [1], organic solar cells[2],display applications[3], lasers [4] and electrochromic materials. Compared with traditional materials, conducting copolymers possess many advantages, such as high conductivity, fast color change[5], redox stability, and easy

processability [6]. Electrochromic polymers can display at least two colors when appropriate voltage is applied to the materials [3].

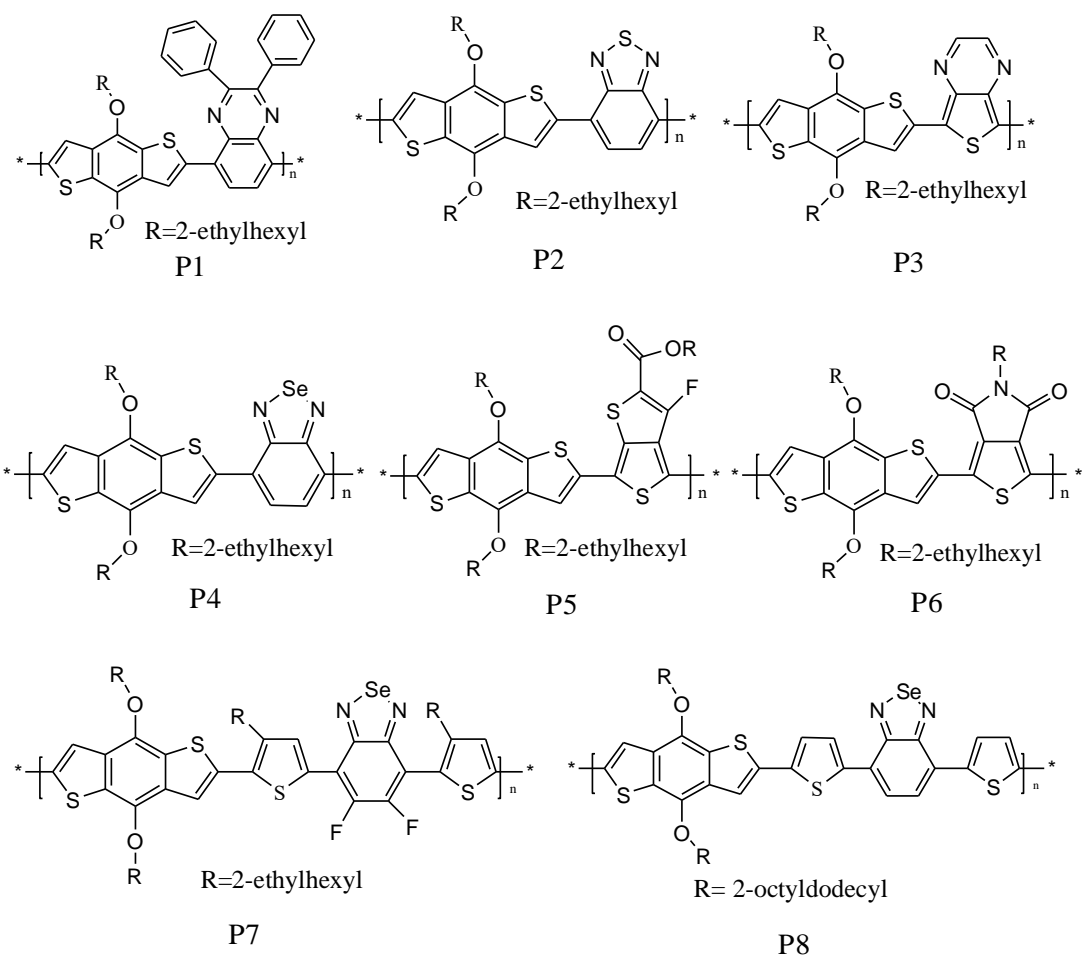
Donor-acceptor method is the most widely used method to tune the band gap of polymers [7]. And band gap is defined as the energy difference between the highest occupied molecular orbital (HOMO) and the lowest unoccupied molecular orbital (LUMO)[8]. The push-pull nature in the backbone is beneficial to the intramolecular charge transfer and electronic delocalization [2]. In detail, the electron donor could increase the valence band energy, promoting the oxidization of the polymers, and the electron acceptor could decrease the conduction band energy, making the reduction easily to happen [9,10]. As a result, the copolymers synthesized with donor-acceptor method have a small band gap. The common electron donor could be thiophene, carbazole, fluorene *etc.*, and the common electron acceptor could be quinoxaline(Qx)[11], benzothiadiazole (BT)[12], thieno[3,4-b]pyrazine (TPz)[13], benzoselenadiazole (BSe) [14] and so on.

Benzo[1,2-b:4,5-b']dithiophene(BDT) is one of the most popular donor units, because it has many good properties [15]. It possesses good planarity owing to connecting two bridged thiophene units, and it has good thermal stability [16], broad absorption and low HOMO level and so on [17]. Moreover, BDT is easily functionalized on the benzene with substituents to tune the solubility of the polymers as well as the HOMO/LUMO energy levels [15]. When aromatic chain is introduced into the donor unit, it can generate an intramolecular charge transfer state, resulting in a low optical bandgap [18]. Since 2008, many D-A type polymers has been prepared taking BDT as the donor unit and varied electron deficient units as the acceptor units, such as Qx (P1), BT (P2), TPz (P3), Bse (P4), thieno[3,4-b]thiophene (P5), thienopyrroledione (P6)[13], 4,7-di(2-ethylhexyl)-2-yl-5,6-difluoro-2,1,3-benzoselenadiazole, (P7) [19], and 4,7-dithien-2-yl-2,1,3-benzoselenadiazole (P8)[14], and the structures of P1-P8 are shown in Scheme 1. The bandgaps and absorption coverages of BDT based polymers could be accurately tuned by the selection of the acceptor units, and absorption edges of which varied from 600 to 1000 nm, the corresponding optical bandgaps ranged from 2.1 to 1.1 eV[13]. Some attractive properites have been found for BDT based polymers, such as promising photovoltaic properties, ideal absorption and electrochemical characterizations, *etc*[13]. However, the electrochromic properties of most of the BDT based polymers have yet not been studied up to present.

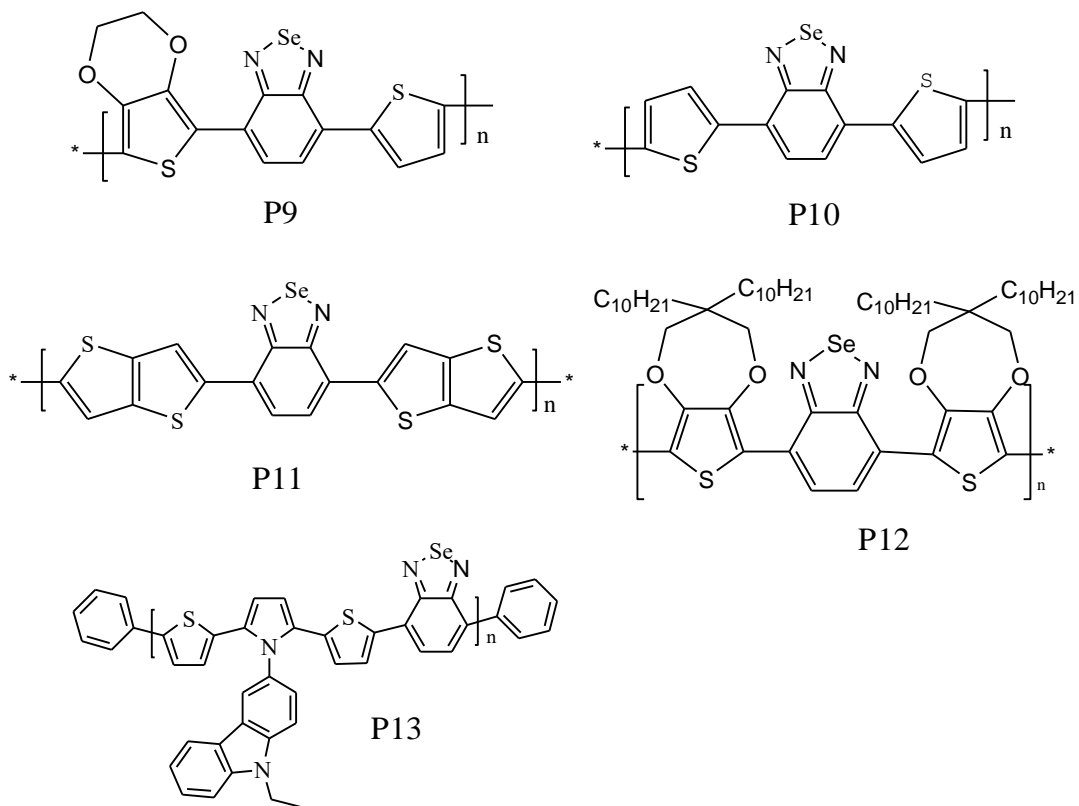
BSe has a analogous structure with that of BT, except the substitute of S atom with Se atom with the molecular structure. Compared with S atom, Se atom is some larger in size and less electronegative[20]. As a resultant, the BSe containing conjugated polymers tends to possess advantageous merits relative to their BT containing analogues, such as low bandgaps, be more effective in spreading the absorption spectrum towards the infrared region, enhanced charge mobilities due to the interchain Se···Se interactions, *etc*[21,22]. Increasing interests have been paid for the construction of D-A type BSe containing electrochromic polymer, which switched between neutral colored state to a highly transmissive oxidized state [23]. As shown in Scheme 2, some D-A type electrochromic polymers have been developed based on BSe as the acceptor unit, and some electron rich group as the donor units, including 3,4-ethylenedioxythiophene (P9)[24] , thiophene (P10)[24], thieno[3,2-b]thiophene (P11)[25],3,3-didecyl-3,4-dihydro-2H-thieno[3,4-b][1,4] dioxepine (P12)[23],and 3-(2,5-di-2-thienyl-1H-pyrrol-1-yl)-9-ethyl-9H-carbazole (P13)[26], respectively. These

polymers usually have excellent electrochromic properties and exhibit robust redox constancy, high coloration efficiency, striking optical contrast and short response period.

Since the bandgaps of BDT containing polymers varied between 2.1 to 1.1 eV, the polymers could be handily obtained in theory with various hues of the RGB color-space in the neutral state. Herein, a BDT based D-A type electrochromic polymer was synthesized taking 4,8-alkoxy substituted benzo[1,2-b:4,5-b']-Dithiophene and electron deficient 4,7-di(2-hexylthiophene)-2-yl-2,1,3-benzoselenadiazole units via Stille coupling reaction (Scheme 3). Although the polymers with similar structures have been synthesized, their applications are still limited to the field of polymer photovoltaics solar cells, and their potential applications as electrochromic materials have remained to be studied systematically[14,22,27]. In the present study, the copolymer containing both BDT and BSe units was prepared and characterized in terms of its electrochromic property. For this purpose, many techniques including cyclic voltammetry(CV), spectroelectrochemistry, kinetics, density functioned theory(DFT), thermal gravimetric analysis, were carried out to have a deep investigation of the electrochromic properties of the copolymer obtained. The results of the present study demonstrated that the copolymer has many attractive electrochromic properties including high contrast in near infrared region (NIR), fast response time and satisfactory color efficiency, which could be a competitive candidate in electrochromic applications.



**Scheme 1.** The molecule structures of some D-A type polymers (P1-P8) based on BDT and different acceptor units.



**Scheme 2.** The molecule structures of some D-A type polymers (P9-P13) employing benzoselenadiazole (BSe) as the electron deficient unit.

## 2. EXPERIMENTAL

### *2.1 Materials*

Chloroform, dichloromethane (DCM), acetone, methanol, ethanol, toluene, ethanol, acetonitrile (ACN), sodium borohydride, selenium dioxide ( $\text{SeO}_2$ ), N-bromosuccinimide (NBS), glacial acetic acid, palladium (II) bis (triphenylphosphine) dichloride ( $(\text{Pd}(\text{PPh}_3)_2\text{Cl}_2)$ ) magnesium sulfate ( $\text{MgSO}_4$ ) are all obtained as analytical grade from Aladdin Co., Ltd and used directly as received. 4,7-dibromo-2,1,3-thiadiazole and (4,8-bis((2-ethylhexyl)oxy)benzo[1,2-b:4,5-b'] dithiophene-2,6-diyl)bis(trimethylstannane) (BBDT) was purchased from Derthon Optoelectronic Materials Science Technology Co., Ltd. (Shenzhen, China). Indium-tin-oxide (ITO) coated glass (sheet resistance:  $< 10 \Omega \cdot \square^{-1}$ , was purchased from Shenzhen CSG Display Technologies, China). Tetrabutylammonium hexafluorophosphate ( $\text{TBAPF}_6$ ) was purchased from Tokyo Chemical Industry Co., LTD. The electrolyte used in this study was the solution of 0.1 M  $\text{TBAPF}_6$  dissolved in ACN.

## *2.2 Instrumentation and methods*

<sup>1</sup> H NMR and <sup>13</sup>C NMR spectroscopy studies were carried out on a Varian AMX 400 spectrometer and tetramethylsilane was used as the internal standard and chloroform was used as the solvent. UV-Vis-NIR spectra and spectroelectrochemistry were conducted on a Varian Cary 5000

spectrophotometer, and a quartz (1 cm × 1 cm × 4.5 cm) was used for the construction of the self-assembly electrolytic cell, in which the counter electrode was a platinum wire (Φ 1 mm), the working electrode was the polymer coated ITO conducting glass, and the reference electrode was an Ag wire (0.02 V vs. SCE). The cyclic voltammetry of the polymers was conducted with IVIUM Vertex.5A. EIS Electrochemical Analyzer in the self-assembly electrolytic cell mentioned above. Colorimetry data of the polymers were also obtained from the UV-vis spectra with the help of chrome analysis software. Digital photographs were taken using a commercially available digital camera with 14 million pixels. The polymer films were obtained by spray-casting polymer solution on the ITO electrode with the covering area was 0.9 cm × 3 cm using an art spray gun. Polymers were dissolved in chloroform to give a concentration of 5 mg/mL, and the insoluble impurities were filtrated away by filtration method. Thermogravimetric analysis and differential thermal gravity was carried out on a NETZSCH STA 499C TG-DSC analyzer. The nanostructure of the polymer films was examined with scanning electron microscopy (SEM). The density functional theory (DFT) calculations were carried out on the DFT level employing the Gaussian 03 program. The ground-state electron density distribution of the highest occupied molecular orbital (HOMO) and lowest unoccupied molecular orbital (LUMO) are calculated on the B3LYP/6-31G level.

## 2.3 synthesis procedures

### 2.3.1 Synthesis of 3,6-dibromobenzene-1,2-diamine

The synthesis process of the 3,6-dibromobenzene-1,2-diamine and other monomers were according to the previous paper [28,29] and be shown in Scheme 3. Firstly, 5.75 g (19.56 mM) of 4,7-dibromo-2,1,3-thiadiazole and 300 mL absolute ethanol were added into a 500 mL three-necked flask in a thermostat water bath. Under electromagnetic stirring at 30 °C, excessive amount of 16 g (422mM) NaBH<sub>4</sub> was added by three times at an interval of 8 h. 48 h later, the mixture was poured directly into appropriate amount of distilled water, in which abundant white floccules were precipitated. Next, it was stirred mechanical for 30 min stirring and filtered by decompression suction, the white solid 3,6-dibromo-1,2-phenylenediamine was afforded <sup>16-19</sup>, and dried for the next step application. <sup>1</sup>H NMR (CDCl<sub>3</sub>, 400 MHz, ppm): δ = 6.84 (s, 2H, Ar H), 3.89 (s, 4H). <sup>13</sup>C NMR (CDCl<sub>3</sub>, δ, ppm): δ = 133.70, 123.24, 109.68.

### 2.3.2. Synthesis of 4,7-dibromobenzo[c][1,2,5]selenadiazole

9.47 g (36.91 mM) of 3,6-dibromo-1,2-phenylenediamine and 200 mL of absolute ethyl alcohol were dissolved in a flask which was heated to 75-90 °C in a water batch. Next, 4.2 g SeO<sub>2</sub> (37.85 mM) was dissolved into appropriate hot water and the solution was added into mixture in the reaction flask slowly. In this process, yellow insoluble substances were produced. Continue to stir and heat after SeO<sub>2</sub> solution was all added with temperature controlled within 75-90 °C. Later, it was refluxed for 2 h [24]. After finishing the reaction, 4,7-dibromo-2,1,3-benzoselenadiazole was afforded from vacuum filtration of the reaction products <sup>20</sup>. It was a yellow solid and was then washed by ethanol for 3 times

and by water for another 3 times. Finally, it was dried in vacuum under 50 °C.  $^1\text{H}$  NMR ( $\text{CDCl}_3$ , 400 MHz, ppm):  $\delta = 7.64$  (s, 2H, Ar H).  $^{13}\text{C}$  NMR ( $\text{CDCl}_3$ ,  $\delta$ , ppm):  $\delta = 158.16, 144.00, 139.30$ .

### 2.3.3. Synthesis of 4,7-bis(4-hexylthiophen-2-yl)benzo[c][1,2,5]selenadiazole (TBSe)

3.41 g (10 mmol) of 4,7-dibromobenzo[c][1,2,5]selenadiazole, 11.0 g (24 mmol) of tributyl(4-hexylthiophen-2-yl)stannane, 0.35 g (0.5 mmol, 5% equiv.) of  $(\text{Pd}(\text{PPh}_3)_2\text{Cl}_2$ , and 160 mL of toluene was added to a single neck round bottom flask, and refluxed under argon atmosphere at 105 °C for 24 hours [24]. After which, toluene was distilled off under reduced pressure distillation. The solid residues was purified by column chromatography with silica gel as the separating medium, and the mobile phase was the mixed solvent of hexane and  $\text{CH}_2\text{Cl}_2$  with the volume ratio of 3:1, and the final product was obtained as red solid.  $^1\text{H}$  NMR (400 MHz,  $\text{CDCl}_3$ )  $\delta$  7.87 (d, 2H), 7.75 (s, 2H), 7.05 (d, 2H), 2.68 (t, 4H), 1.69 (m, 4H), 1.45-1.25 (m, 12H), 0.90 (t, 6H).  $^{13}\text{C}$  NMR (101 MHz,  $\text{CDCl}_3$ )  $\delta$  158.16, 144.00, 139.31, 128.87, 127.38, 125.75, 121.86, 31.75, 30.67, 30.51, 29.11, 22.69, 14.19.

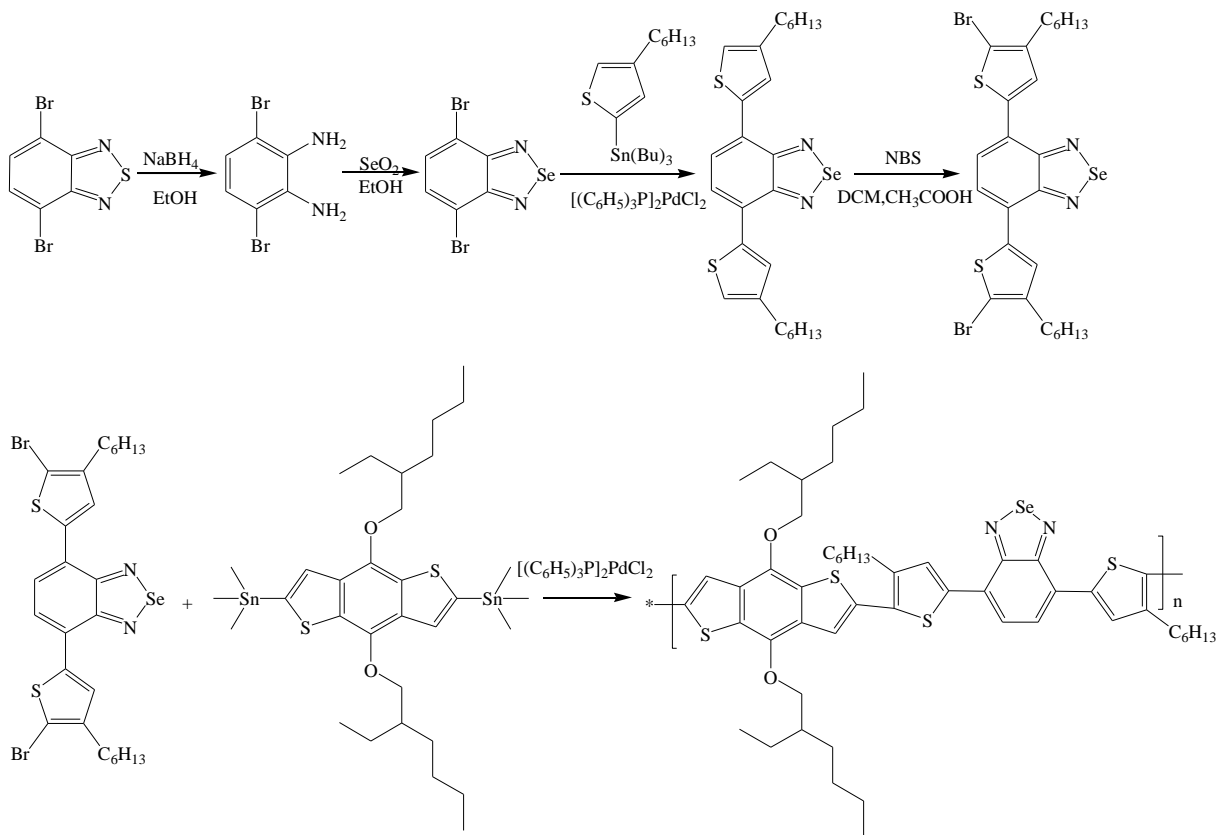
### 2.3.4. Synthesis of 4,7-bis(5-bromo-4-hexylthiophen-2-yl)benzo[c][1,2,5]selenadiazole (BTBSe)

15.5 g (29.1 mmol) of TBSe was dissolved in 200 mL of mixed solvent consisting of  $\text{CH}_2\text{Cl}_2$  and glacial acetic acid with the volume ratio of 1:1, and the solution was added to a three-neck round bottom flask. 9.9431 g of NBS (2.4 equiv) was dissolved in  $\text{CH}_2\text{Cl}_2$ . The BHBS solution was stirred magnetically and be heated to 70 °C, at the same time, the NBS solution was added dropwise to the above solution[19]. The reaction was continued for 24 hours, after which, the mixture was poured into the 600 mL of water, and the organic phase were rinsed with 200 mL of saturated  $\text{Na}_2\text{SO}_3$  for 4 times and extracted with chloroform. The organic part was dried with  $\text{MgSO}_4$ , and then the solvent was distilled off. Column chromatography was used to get pure product with silica gel as the separating medium, and the mobile phase was mixed solvent (hexane/dichloromethane, 1:1, v/v).  $^1\text{H}$  NMR (400 MHz,  $\text{CDCl}_3$ )  $\delta$  7.52(s, 2H), 7.44(s, 2H), 2.55(t, 4H), 1.63(m, 4H), 1.34(m, 12H), 0.91(t, 6H).  $^{13}\text{C}$  NMR (101 MHz,  $\text{CDCl}_3$ )  $\delta$  161.97, 147.10, 143.23, 131.98, 130.89, 129.11, 116.87, 36.32, 34.43, 34.27, 33.69, 27.33, 18.84.

### 2.3.5. Synthesis of poly(benzo[1,2-b:4,5-b']dithiophene-benzoselenadiazole)(PBDTBS)

0.7723 g (1 mM) of BDT, 0.671 g (1 mM) of **BTBSe** and 0.02804 g (4% equiv.) of  $\text{Pd}(\text{PPh}_3)_2\text{Cl}_2$  were dissolved in 100 mL of toluene, and be added to a 250 mL round bottom flask[19]. The mixture solution was heated to 105 °C and maintained reflux for 24 h under argon atmosphere. When the reaction was completed, the toluene was distilled off and methanol was added to the flask, the solid precipitation was obtained by pumping filtration, and the crude product was extracted with methanol for 24 hours until the solution in Soxhlet extractor was transparent. Then it was extracted with acetone for 24 hours until the solution was transparent, too. The purified polymer PBDTBS was obtained as deep green solid with 75% yield.  $^1\text{H}$  NMR (400 MHz,  $\text{CDCl}_3$ )  $\delta$  8.06-7.58 (m, 4H), 7.39-

7.01 (m, 2H), 4.44-3.86 (m, 4H), 3.12-2.75 (m, 4H), 2.00-1.23 (m, 34H), 1.23-0.83 (m, 18H). Molecular weight test information was obtained by GPC measurement using PMMA (with known molecular) dissolved in THF as standard: ( $M_n=16.7$ ,  $M_w=25.6$ , PDI=1.53).



**Scheme 3.** Synthetic routes of the monomers and the copolymer of PBDTBS.

### 3. RESULTS AND DISCUSSION

#### 3.1 Electrochemistry

The copolymer was dissolved in  $\text{CHCl}_3$ , then the solution was sprayed on the ITO conducting glass, after the solvent was evaporated, the copolymer film coated on ITO electrode was obtained. Cyclic voltammograph was conducted and the data are shown in Fig. 1. When the voltage was swept from -2.0 V to 2.0 V, redox peaks were found for both the anodic doping and the cathodic reduction reactions. The p-doping peak was located at 0.81 V, which is relatively low, demonstrating that the copolymer could be easily oxidized. Since the HOMO energy level of the polymer approximately equal to that of the donor units within the polymer, which could be easily obtained from the value of the onset oxidation potential. The higher of the HOMO energy level is, the lower onset oxidation potential could be observed [24]. In this case, benzo[1,2-b:4,5-b'] dithiophene derivative could be a good candidate as electron donor. The peaks of n-doping/n-dedoping are located at -1.12 V and -1.32 V. BSe is a good electron acceptor and can get the electron easily, so the position of reduction peak is

relatively low. The onset oxidation potential ( $E_{onset}$ ) is calculated from CV graphs by taking the intersection of baseline and tangent of oxidization peak, and the value is 0.62 V. At the meantime, the onset reduction potential in the dedoping process is -0.69 V, as shown in Fig.1, and the electrochemical band gap of PBDTBS was calculated to be 1.31 V. The  $E_{onset}$  is used to calculate the HOMO level in the following discussion.

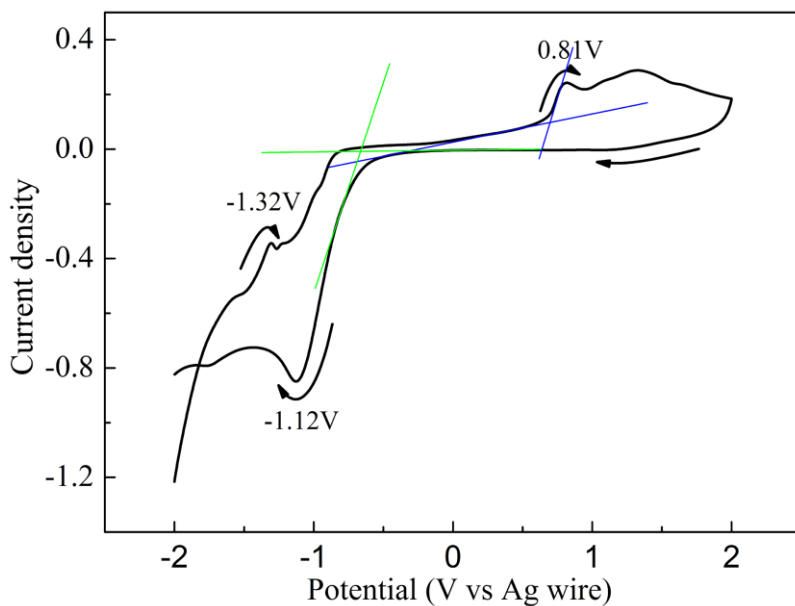


**Figure 1.** Cyclic voltammogram(CV) of the copolymer PBDTBS, which was conducted in monomer free 0.2 M 0.1 M TBAPF<sub>6</sub> dissolved in CAN, and the scan rate was 100 mV/s.

### 3.2. Optical absorption spectra of copolymer solution and film

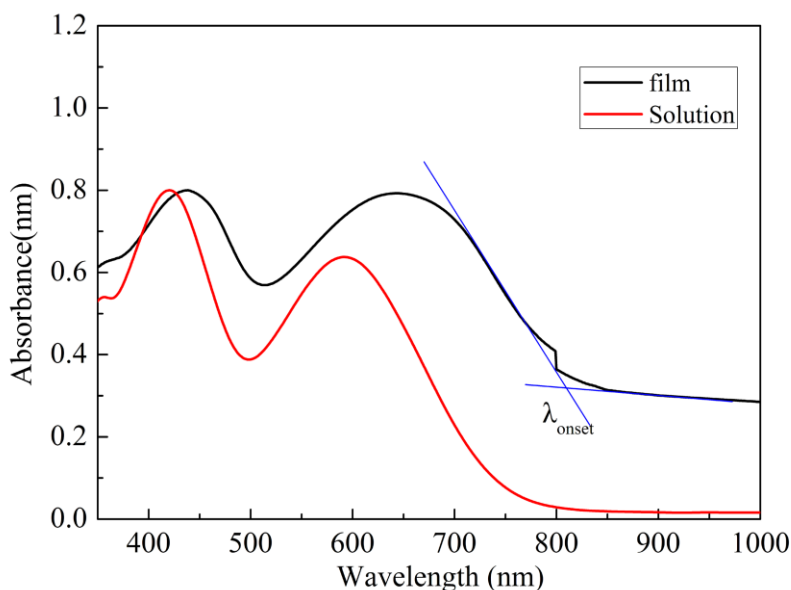


**Figure 2.** The absorption spectra of the PBDTBS solution (dissolved in chloroform) and its film spray coated on the ITO glass.

Optical absorption spectra of PBDTBS solution (dissolved in chloroform) and film and their photos are shown in Fig. 2. For PBDTBS solution, there are two peaks located at 420 nm and 592 nm, which could be ascribed to the  $\pi-\pi^*$  transition and intramolecular charge transfer, respectively [30]. The peak valley is located at 498 nm, as we know, the light between 500 nm and 560 nm is green light, so the color of the solution is darklategrey. Similar with PBDTBS solution, PBDTBS film also displays two absorption peaks at 437 nm and 643 nm, respectively. The depth of the peak valley of the copolymer film is lower than that of the solution, which suggests that the absorbance of green light for copolymer film is higher than solution, so the film displays a greyish-green color. Compared with PBDTBS solution, PBDTBS film has a significant bathochromic shift, because the structure of the film is compact, and the  $\pi-\pi$  stacking in the film can enhance the inter-chain interaction, lowering the absorption energy consequently [31, 32].

### 3.3. Spectroelectrochemistry

When the potential is applied to the ITO conducting glass from -0.30 V to 1.24 V, the copolymer film turns from neutral state to oxidized state. As shown in Fig. 3, in neutral state, there are two absorption peaks located at 432 nm and 636 nm due to the  $\pi-\pi^*$  transition and intramolecular charge transfer and the color of copolymer is greyish-green [24]. With the potential increasing, the absorption peaks in visible region decrease, while the peak valley in green region increases. At last, the absorption in visible region is nearly equal, so the film color turns to a darkgrey color. In addition, there are two new peaks located at 850 nm and a much longer wavelength (around at 1400 nm), which can be ascribed to the formation of polarons and bipolarons [31, 32]. When the potential is 1.24 V, the absorbance of polarons reached to the maximum, while the peak of bipolarons increases with the increase of potential. The reason is that bipolaron is more stable than polaron in a strong field [34].

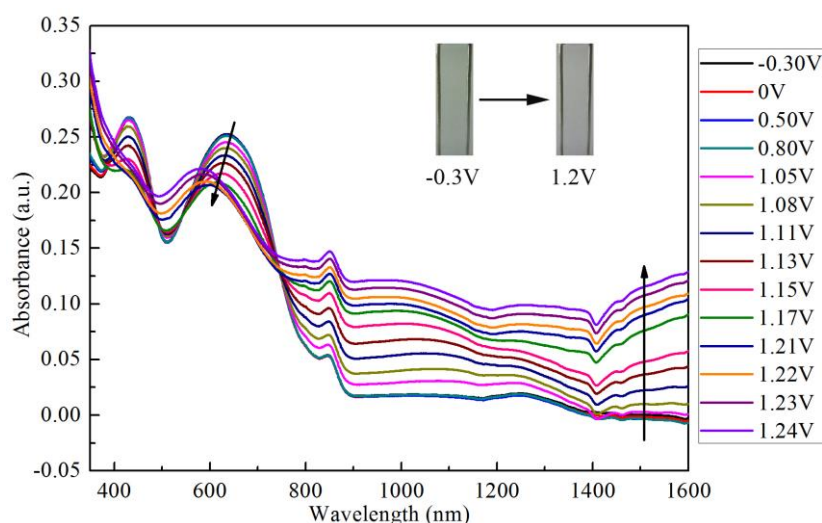


**Figure 3.** Spectroelectrochemistry graphs and photos of PBDTBS at different potentials exerted on the polymer coated ITO electrode. The film was immersed in monomer free electrolyte and the potentials biased on it was between -0.30 V versus 1.24 V.

According to the spectroelectrochemistry graph in neutral state, we can get the onset edge of the optical absorption wavelength ( $\lambda_{\text{onset}}$ ) by taking the intersection of baseline and the tangent of the peak, and the  $\lambda_{\text{onset}}$  of PBDTBS is 802 nm. According to the previous paper, we can get

the value of optical band gap ( $E_g$ ) and HOMO/LUMO energy levels by the formulas  $E_g=1241/\lambda_{\text{onset}}$ ,  $E_{\text{HOMO}}=-e(E_{\text{onset}}+4.4)$  and  $E_{\text{LUMO}}=E_{\text{HOMO}}+E_g$ , respectively [35, 36]. The  $E_g$ ,  $E_{\text{HOMO}}$  and  $E_{\text{LUMO}}$  values of PBDTBS are 1.55 eV, -5.02 eV, -3.47 eV, respectively. Band gap is relevant with the energy consumption during the doping and dedoping process, and if the band gap is small, it means the energy cost in transferring from HOMO level to LUMO level is low. The band gap of PBDTBS is low, which is attributed to the ideal matching of the donor unit and the acceptor unit employed in this work.

### 3.4 Density functional theory calculation(DFT)

The frontier molecular orbital of the monomer was calculated by Gauss 09 with the basic set

3-21 G. Fig. 4 shows the molecular orbital diagrams of HOMO and LUMO of PBDTBS repeating unit, where  $\theta_1$  is the dihedral angle between benzo[1,2-b:4,5-b']dithiophene and thiophene,  $\theta_2$  and  $\theta_3$  are the dihedral angles between benzoselenadiazole and two thiophenes. Although we can't get the simulation graphs of PBDTBS, the repeating unit has the similarity with their copolymer in dihedral angle, and the values of  $\theta_1$ ,  $\theta_2$  and  $\theta_3$  are  $0.07^\circ$ ,  $0.13^\circ$  and  $0.10^\circ$ , respectively. They are all very small, and indicated that the copolymer has a perfect planar structure, which is beneficial to the electron delocalization and  $\pi$ - $\pi$  stacking. In addition, the phenomenon that there is a bathochromic shift for the copolymer film absorption peak compared with copolymer solution is verified by the simulation. Furthermore, we also investigate the structure of side chain.  $\theta_4$  is the dihedral angle between backbone and alkyl chain, and  $\theta_5$  is the dihedral angle between backbone and alkoxy chain. The values of  $\theta_4$  and  $\theta_5$  are  $0.06^\circ$  and  $88.23^\circ$ . The alkyl chain is nearly in the same plane with the backbone, while the alkoxy chain is nearly perpendicular with the backbone. The branched side chains are beneficial to the solubility of the polymer.

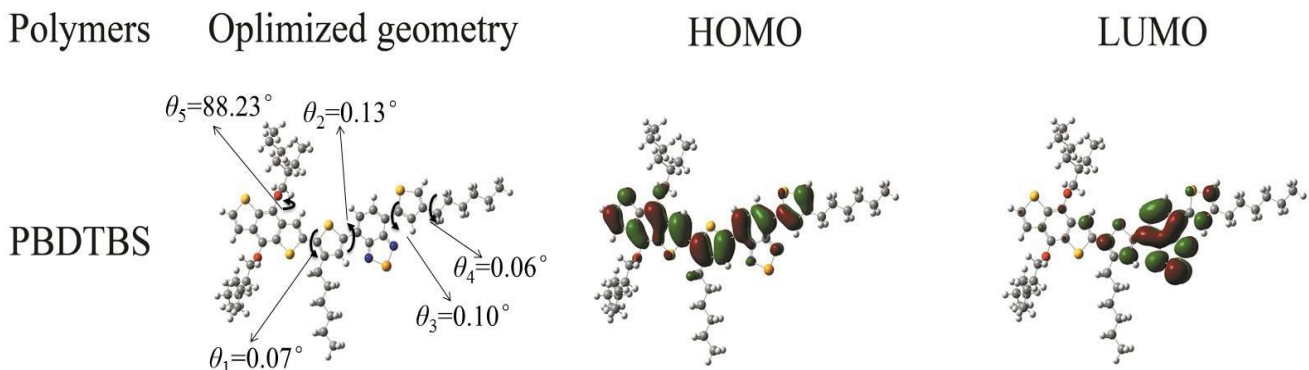


**Figure 4.** Molecular orbital diagrams of HOMO and LUMO of PBDTBSrepeating unit calculated on the B3LYP/6-31G level.

### 3.5. Electrochromic switching of PBDTBS

Kinetic experiment is an important method to evaluate the switching property of the copolymer. When the potential was interchanged between -0.30 V and 1.24 V, we could get the graph that transmittance changes with the potential, where the interval in the experiment is 4 s. Optical contrast ( $\Delta T\%$ ) is defined as the transmittance difference between neutral state and oxidized state[37]. As shown in Fig. 5, the optical contrast is 14.0 % at 450 nm, 9.0 % at 670 nm and 30.7 % at 1560 nm. The  $\Delta T\%$  in near infrared region is much higher than the  $\Delta T\%$  in visible region, indicating that it can be applied to the near infrared region.

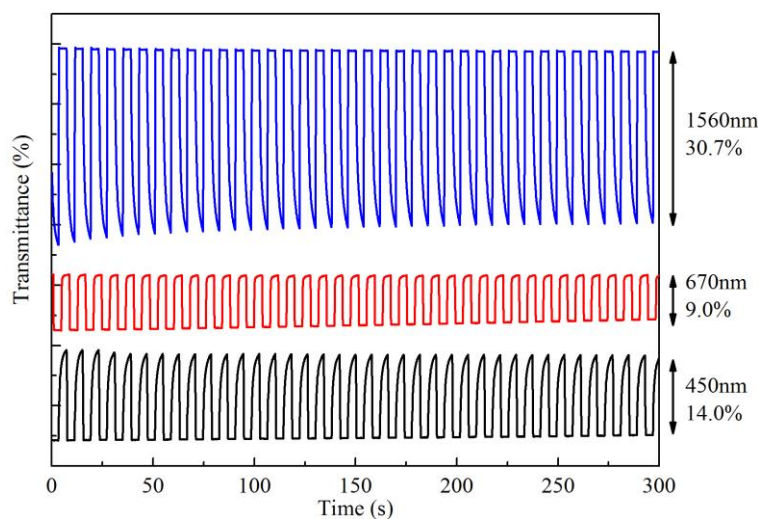


**Figure 5.** Electrochromic switching of PBDTBS at different wavelengths.

**Table 1.** The optical contrast, response time, coloration efficiency of PBDTBS at different wavelengths.

copolymers	$\lambda$ nm	$\Delta T\%$ %	response time( $t_{95\%}$ ) s	coloration efficiency ( $\eta$ ) $\text{cm}^2 \cdot \text{C}^{-1}$
<b>PBDTBS</b>	450	14.0	2.95	60.61
	670	9.0	0.90	84.60
	1560	30.7	2.85	135.84

Another parameter in kinetic experiment is response time( $t_{95\%}$ ), which is defined as the time from neutral state to the 95 % of the oxidized state, while the reason is that human eyes are not very sensitive to color change [37, 38]. The response time of PBDTBS is 2.95 s at 450 nm, 0.90 s at 670 nm and 2.85 s at 1560 nm. Coloration efficiency ( $\eta$ ) is the ratio of change in optical density to the charge density per cycle [38], and is calculated as the following equations [40].

$$\eta = \Delta OD / \Delta Q$$

$$\Delta OD = \lg(T_b/T_c)$$

$$\Delta Q = Q/A$$

where  $\Delta OD$  is the change in optical density,  $\Delta Q$  is the charge density injected to the film per cycle.  $T_b$ ,  $T_c$  are transmittances in neutral states and oxidized states, respectively.  $Q$  was integrated according to the multi-potential steps diagram. The coloration efficiency of PBDTBS are  $60.61 \text{ cm}^2 \cdot \text{C}^{-1}$  at 450 nm,  $84.60 \text{ cm}^2 \cdot \text{C}^{-1}$  at 670 nm and  $135.84 \text{ cm}^2 \cdot \text{C}^{-1}$  at 1560 nm. Although the coloration efficiency isn't much high in the visible region, the coloration efficiency in infrared region is much higher than visible region. These parameters are summarized in Table 1.

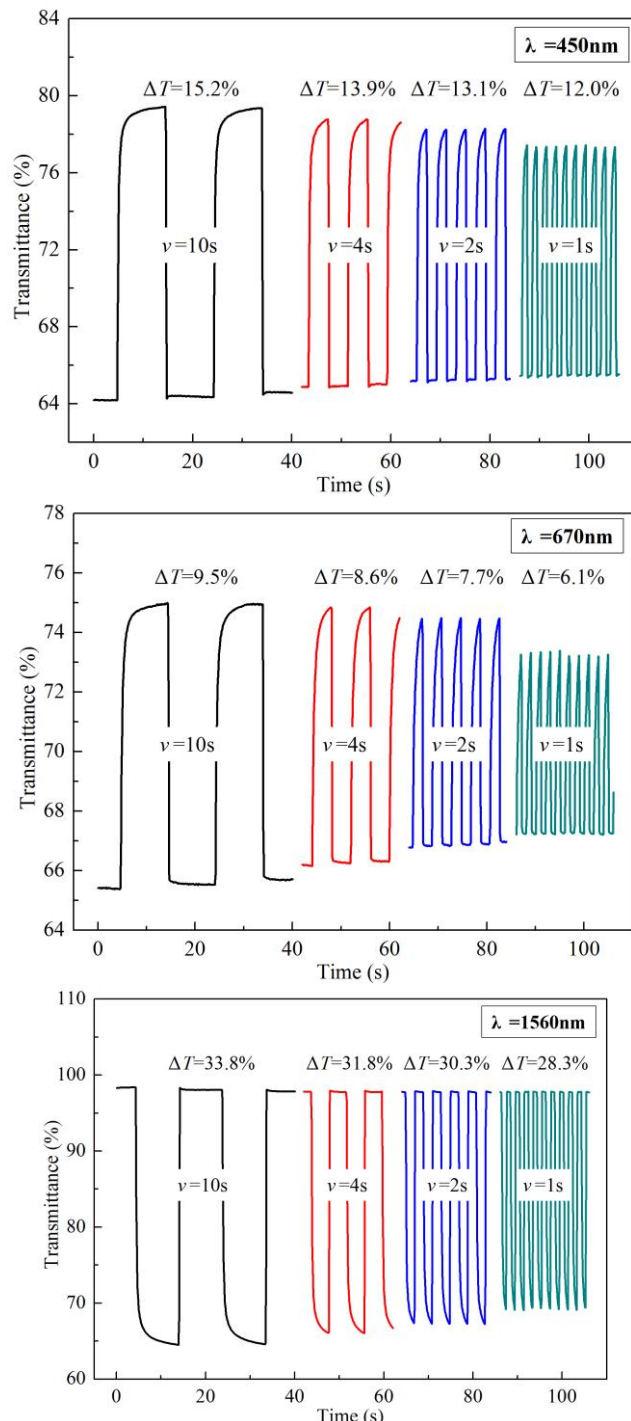


**Figure 6.** Electrochromic switching of PBDTBS at different wavelengths with an interval of 10 s, 4 s, 2 s and 1 s, respectively.

In addition, we also investigate the effect of time intervals on the optical contrast. When the interval changes from 10 s to 4 s, 2 s and 1 s, the  $\Delta T\%$  drops from 15.2 % to 12.0 % at 450 nm, from 9.5 % to 6.1 % at 670 nm, from 33.8 % to 28.3 % at 1560 nm, and the decrease isn't significant. Compact structure is unbeneficial to the ion-solvent ingress and egress [39], while the copolymer backbone has a good planar structure, which is good to  $\pi$ - $\pi$  stacking property and compact structure, so the phenomenon may be ascribed to the side chain. The alkoxy chain is nearly perpendicular with the backbone, having a large branch structure, and the branched chain stretches the distance between adjacent backbones, which is good for the transfer of ion-solvent.

### 3.6. Colorimetry

Colorimetry experiment was carried out to characterize the color changes of the copolymer at different potentials. In our experiments, we adopt CIE 1976  $L^*a^*b^*$  Color Space, where  $L^*$  represents the lightness ranged from 0 to 100 (black to white),  $a^*$  represents how much red versus green, and  $b^*$  represents how much yellow versus blue [39]. The lightness as a function of the applied voltage is shown in Fig. 7. With the potential increasing, the lightness doesn't change so much under 0.8 V, and when the potential is up to 0.8 V, there is an increase, meaning that the copolymer film turns lighter.

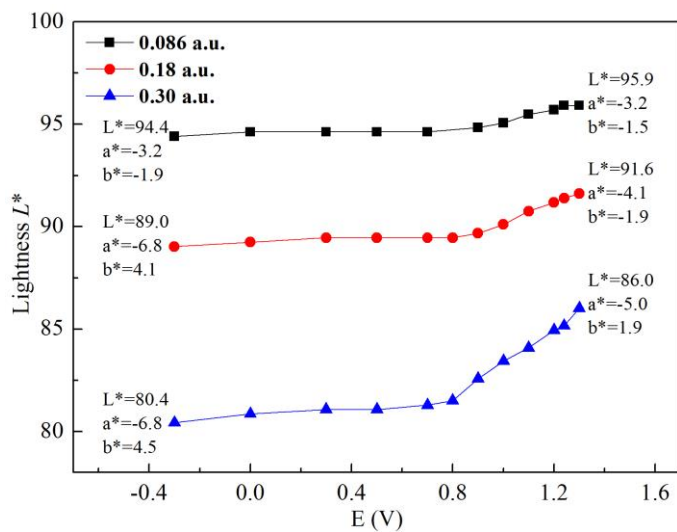


**Figure 7.** Lightness as a function of the applied voltage for PBDTBS.

In addition, when the film is thick, the value of lightness is smaller than the thinner film. For example, when the thickness changes from 0.086 a.u. to 0.18 a.u. and to 0.30 a.u. (measured at 432 nm), the lightness changes from 94.4 to 89.0 and to 80.4 in oxidized state, and from 95.9 to 91.6 and to 86.0 in neutral state. When the film is thin, the absorbance of light is little, so the film is light. As a whole, the  $a^*$  turns bigger, while the  $b^*$  turns smaller, so the color changes from greyish-green to transparent darkgrey. However, due to the change of  $a^*$  and  $b^*$  isn't very significant, the color isn't very significant, either.

### 3.7. Thermal gravimetric analysis

Thermal stability is necessary for the copolymer, because if the copolymer isn't stable, many applications will be limited. Fig. 8 demonstrates the thermal gravimetric (TG) and differential thermal gravity (DTG) of PBDTBS, both are the functions of the temperature with a heating rate of 10 °C/min. The mass of the polymer remained unchanged up to 327 °C, and the maximum degradation rate occurred at 350 °C, which was followed by another maximum degradation point at 500 °C. More than 50% mass percent was remained at 800 °C from the TG curve, which suggested that the polymer had enough thermal stability [41]

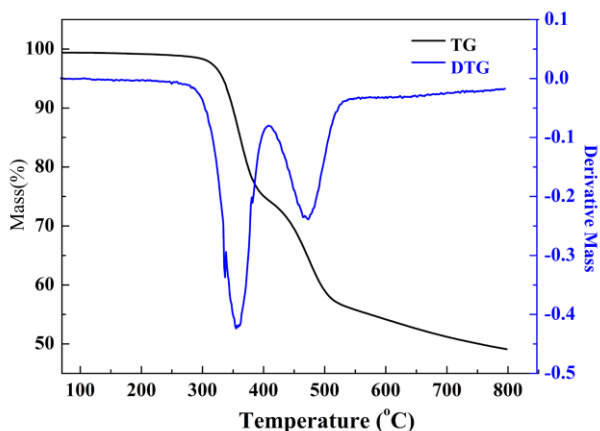


**Figure 8.** TG and DTG curves of PBDTBS conducted under nitrogen atmosphere with a heating rate of 15 K/min.

## 4. CONCLUSION

One copolymer taking benzo[1,2-b:4,5-b']dithiophene as electron donor and benzoselenadiazole as electron acceptor, was synthesized successfully. When the copolymer is oxidized, the copolymer film changes from greyish-green to darkgrey. The band gap of the copolymer is 1.55 eV, and the optical contrast, response time and coloration efficiency at 1560 nm are 30.7%, 2.85 s,  $135.84 \text{ cm}^2 \cdot \text{C}^{-1}$ , respectively. The problem we met in the experiments is the poor solubility, leading to the operation difficult, so the following researchers can introduce long and branched side chain to the backbone to enhance the solubility. In summary, it could be a candidate for the electrochromic application.

## SUPPORTING INFORMATION:

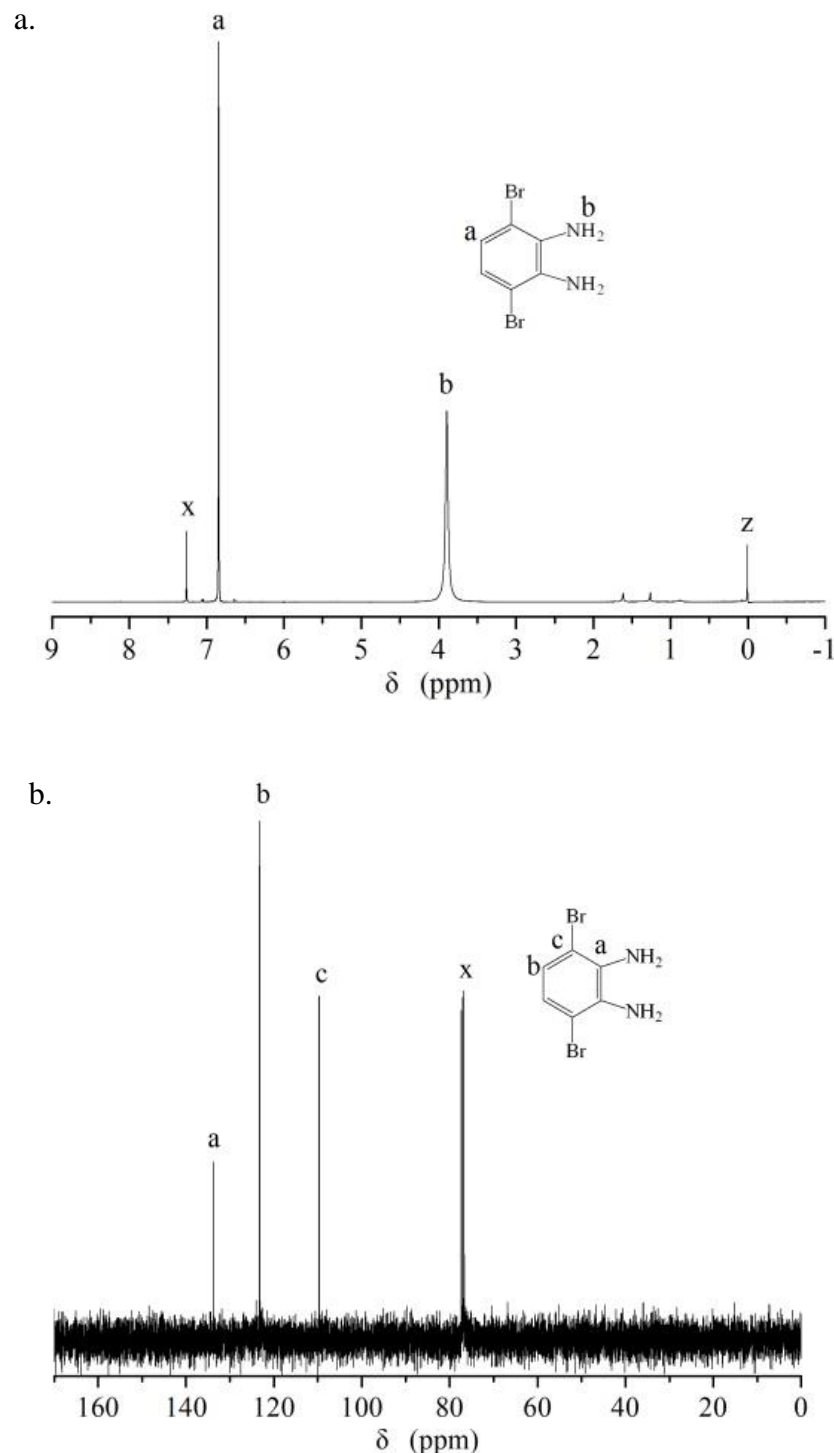


**Fig. S1.** (a)  $^1\text{H}$  NMR spectrum and (b)  $^{13}\text{C}$  NMR spectrum of 3,6-dibromobenzene-1,2-diamine in  $\text{CDCl}_3$ , x, z denote the peaks of chloroform and tetramethylsilane in **Fig. S1(a)**, x donates the peak of chloroform in **Fig. S1(b)**.

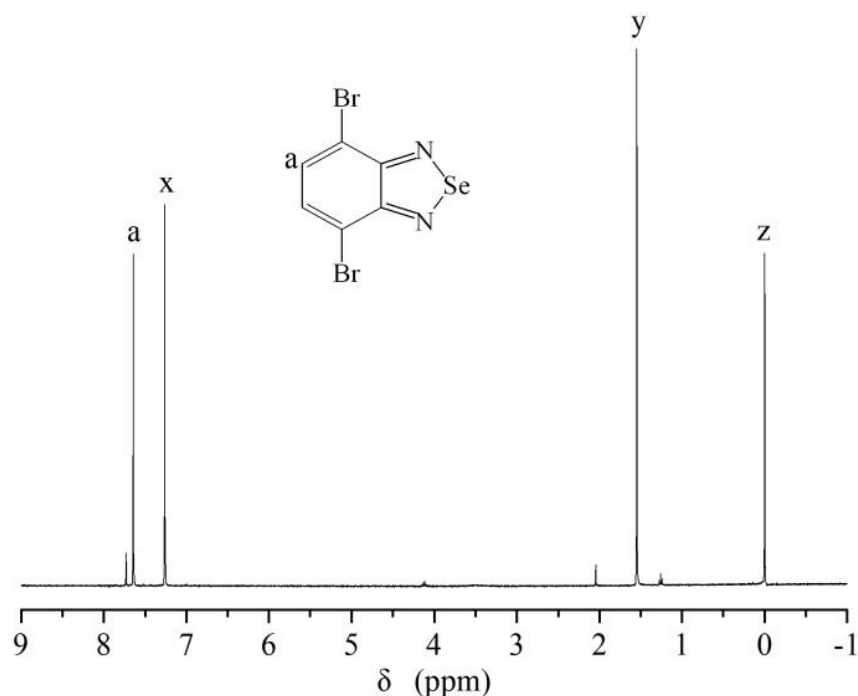
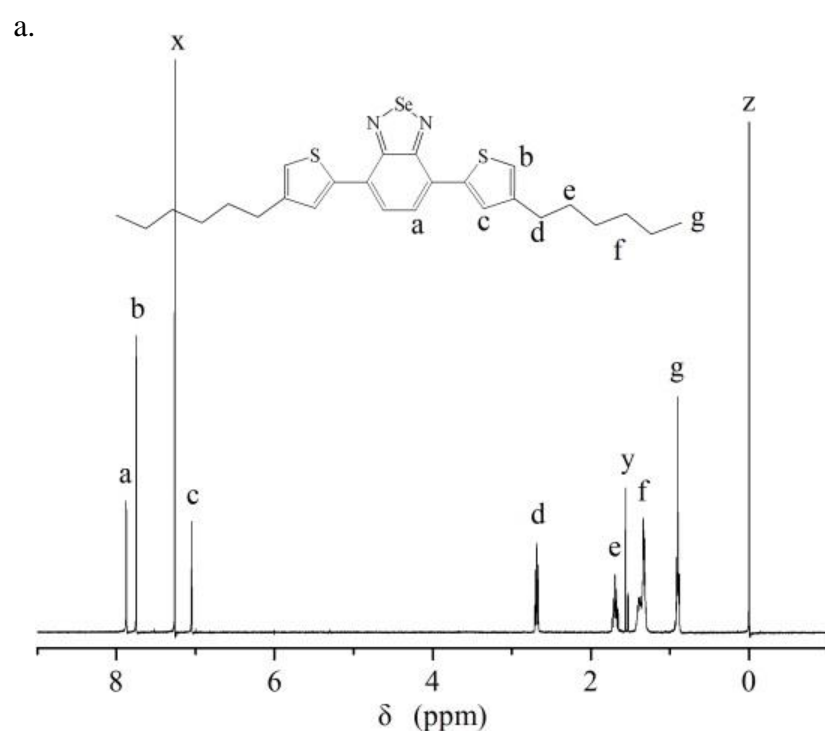


**Fig. S2.**  $^1\text{H}$  NMR spectrum of 4,7-dibromobenzo[c][1,2,5]selenadiazole in  $\text{CDCl}_3$ , x, y, z denote the peaks of chloroform,  $\text{H}_2\text{O}$  and tetramethylsilane.



b.

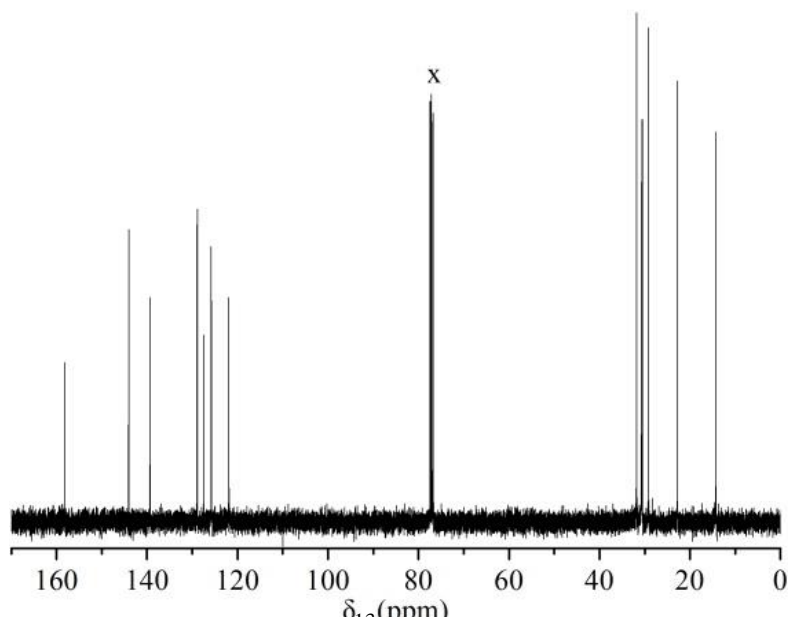
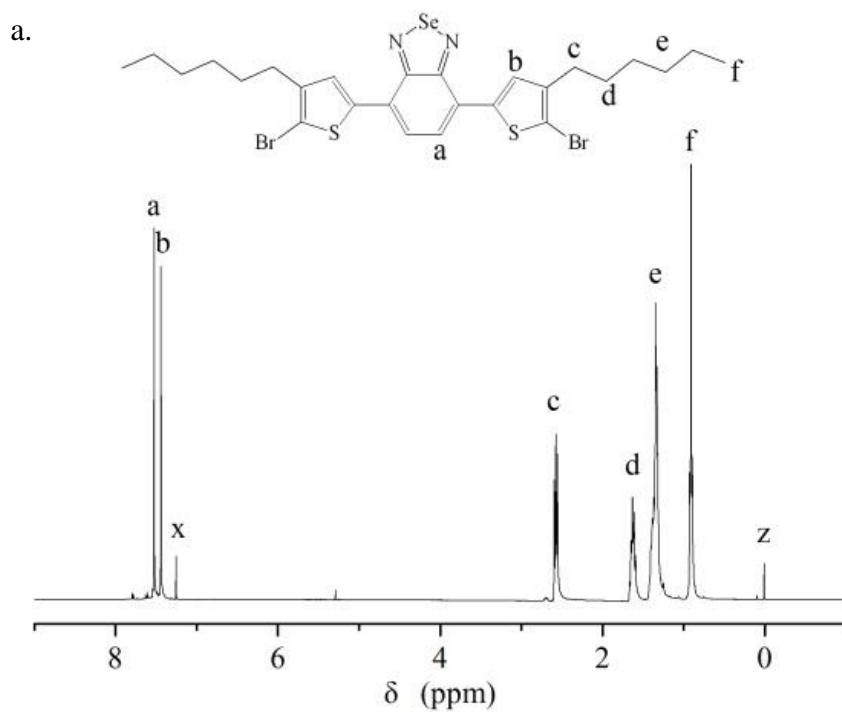


**Fig. S3.** (a)  $^1\text{H}$  NMR spectrum and (b)  $^{13}\text{C}$  NMR spectrum of 4,7-bis(4-hexylthiophen-2-yl)benzo[c][1,2,5]selenadiazole in  $\text{CDCl}_3$ , x, y, z denote the peaks of chloroform,  $\text{H}_2\text{O}$  and tetramethylsilane in **Fig. S3(a)** and x donates the peak of chloroform in **Fig. S3(b)**.



b.

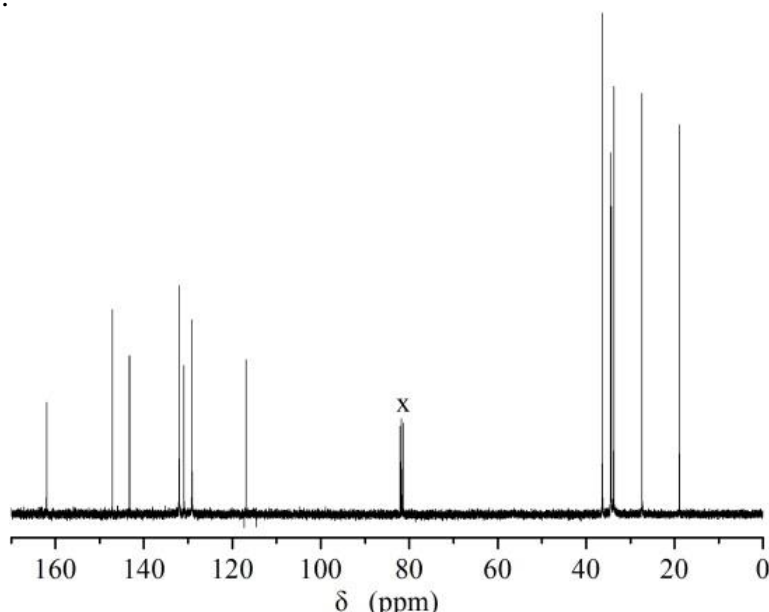


**Fig. S4.** (a) <sup>1</sup>H NMR spectrum and (b) <sup>13</sup>C NMR spectrum of 4,7-bis(5-bromo-4-hexylthiophen-2-yl)benzo[c][1,2,5]selenadiazole in CDCl<sub>3</sub>, x, y, z donate the peaks of chloroform, H<sub>2</sub>O and tetramethylsilane in **Fig. S4(a)**, x donates the peak of chloroform in **Fig. S4(b)**.

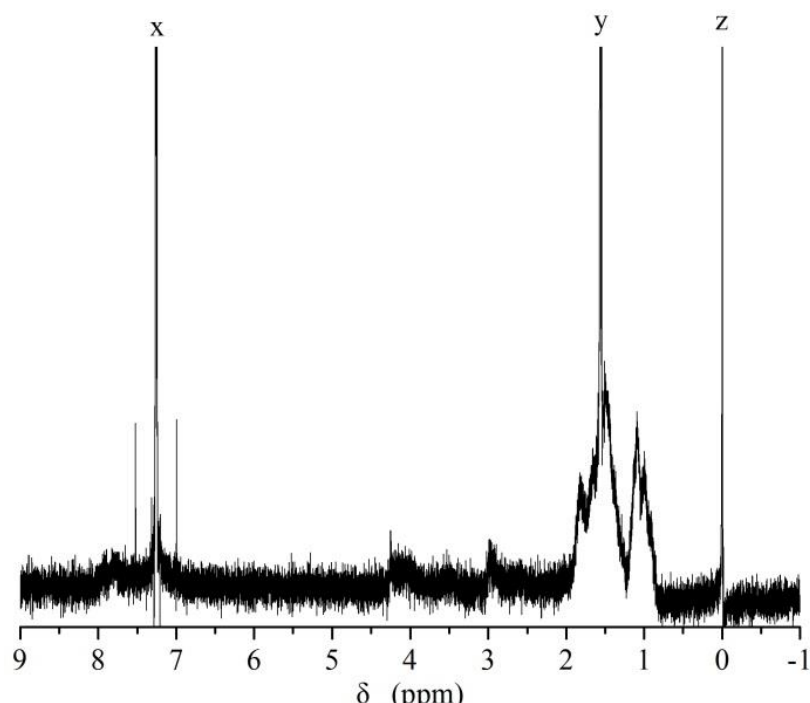


**Fig. S5.** <sup>1</sup>H NMR spectrum of poly(benzo[1,2-b:4,5-b']dithiophene-benzoselenadiazole) (**PBDTBS**) in CDCl<sub>3</sub>, x, y, z donate the peaks of chloroform, H<sub>2</sub>O and tetramethylsilane.

#### ACKNOWLEDGEMENTS

The work was financially supported by the National Natural Science Foundation of China (31400044 and 51473074), and the Natural Science Foundation of Shandong Province (ZR 2014JL009).

## References

1. A.P. Kulkarni, C.J. Tonzola, A. Babel, S.A. Jenekhe. *Chem Mater.*, 16 (2004) 4556.
2. X. Liu, Y. Sun, B.B.Y. Hsu, A. Lorbach, L. Qi, A.J. Heeger. *J. Am. Chem. Soc.* 136 (2014) 5697.
3. R.J. Mortimer, A.L. Dyer, J.R. Reynolds. *Displays.*, 27 (2006) 2.
4. A.J. Heeger. *Solid State Commun.*, 107 (1998) 673.
5. G. Xu, J. Zhao, J. Liu, C. Cui, Y. Hou, Y. Kong., *J. Electrochem. Soc.* 160 (2013) G149.
6. X. Cheng, J. Zhao, C. Cui, Y. Fu, X. Zhang. *J. Electroanal. Chem.*, 677 (2012) 24.
7. G. Gunbas, L. Toppare. *Chem. Commun.*, 48 (2012) 1083.
8. G. Yu, A.J. Heeger. *Synthetic Met.*, 85 (1997) 1183.
9. S. Celebi, A. Balan, B. Epik, D. Baran, L. Toppare. *Organic Electronics.*, 10 (2009) 631.
10. C. DuBois, K.A. Abboud, J.R. Reynolds. *J. Phys. Chem.B.*, 108 (2004) 8550.
11. H.C.Chen, Y.H. Chen, C.C. Liu, Y.C. Chien, S.W. Chou, P.T. Chou, *Chem. Mater.*, 24 (2012) 4766.
12. P.M.Beaujuge, S.V.Vasilyeva, D.Y.Liu, S. Ellinger, T.D. McCarley, J.R. Reynolds, *Chem. Mater.*, 24 (2012) 255.
13. J.H.Hou, M.H.Park, S.Q.Zhang, Y.Yao, L.M.Chen, J.H. Li, Y.Yang, *Macromolecules.*, 41 (2008) 6012.
14. E.Zhou, J.Cong, K.Hashimoto, K.A. Tajima, *Macromolecules*, 46 (2013) 763.
15. X. Zhang, L. Chen, G. Wang, Z.G. Zhang, Y. Li, P. Shen, *Synthetic. Met.* 211 (2016) 121.
16. X.Zhou, X. Li, Y. Liu, R. Li, K. Jiang, J. Xia, *Org. Electron.*, 25 (2015) 245.
17. Q. Fan, M. Li, P. Yang, Y. Liu, M. Xiao, X. Wang, *Dyes Pigments.*, 116 (2015) 13.
18. N. Yin, L. Wang, Y. Ma, Y. Lin, J. Wu, Q. Luo, *Dyes Pigments*, 120 (2015) 299.
19. P.Shen, H.J. Bin, Y. Zhang, Y.F. Li, *Poly. Chem.*, 5 (2014) 567.
20. Y. Lei, H. Li, X. Huang, J. Chen, M. Liu, W. Gao, *Tetrahedron.*, 71 (2015) 3453.
21. J.H. Kim, J.B. Park, S.A. Shin, M.H. Hyun, D.H. Hwang, *Polymer*, 55 (2014) 3605.
22. S.A. Shin, J.B. Park, J.H Kim, D.H. Hwang. *Synthetic. Met.*, 172 (2013) 54.
23. M. İçli, M. Pamuk, F. Algi, A.M. Önal, A. Cihaner, *Chem. Mater.*, 22(2010) 4034.
24. A. Cihaner, F. Algi.. *Adv. Funct. Mater.*, 18 (2008) 3583.
25. S.Toksabay, S.O.Hacioglu, N.A.Unlu, A. Cirpan, *Polymer*, 55 (2014) 3093.
26. F.B.Koyuncu, E.Sefer, S.Koyuncu, E. ozdemir, *Polymer*, 52 (2011) 5772.
27. W.J. Tang, X.W. Chen, Y.P. Zou, B. Liu, H. Zhong, C.Y. Pan, *J. Appl. Polym. Sci.*, 128 (2013) 3678.
28. D. Baran, G. Oktem, S. Celebi, L. Toppare. *Macromol. Chem. Phys.*, 212 (2011) 799.
29. Y. Tsubata, T. Suzuki, T. Miyashi, Y. Yamashita. *J. Org. Chem.*, 57 (1992) 6749.
30. Y. Liu, M. Wang, J. Zhao, C. Cui, J. Liu. *RSC Advances.*, 4 (2014) 52712.
31. C.L. Chochos, S.A. Choulis. *Prog. Polym. Sci.*, 36 (2011) 1326.
32. W.T. Neo, L.M. Loo, J. Song, X. Wang, C.M. Cho, H.S.O. Chan, *Polym. Chem.* 4 (2013) 4663.
33. S. Debnath, A. Bedi, S.S. Zade. Thienopentathiepine: sulfur containing fused heterocycle for conjugated systems and their electrochemical polymerization. *Polym. Chem.*, 6 (2015) 7658.
34. P. Acioli. *J. Mol. Struc. THEOCHEM.*, 539 (2001) 45.
35. W. Yang, J. Zhao, C. Cui, Y. Kong, X. Zhang, P. Li. *J. Solid. State. Electrochem.*, 16 (2012) 3805.
36. G. Xu, J. Zhao, C. Cui, Y. Hou, Y. Kong. *Electrochim. Acta.*, 112 (2013) 95.
37. H. Zhao, D. Tang, J. Zhao, M. Wang, J. Dou. *RSC Advances.*, 4 (2014) 61537.
38. Z. Xu, M. Wang, J. Zhao, C. Cui, W. Fan, J. Liu. *Electrochim. Acta.* 125 (2014) 241.
39. C.M. Amb, A.L. Dyer, J.R. Reynolds. *Chem Mater.*, 23 (2011) 397.
40. B. Wang, J. Zhao, C. Cui, M. Wang, Z. Wang, Q. He. *Opt Mater.*, 34 (2012) 1095.
41. D. Zhang, M.Wang, X.L.Liu, J.S. Zhao, *RSC Advance.*, 6 (2016) 94014.